

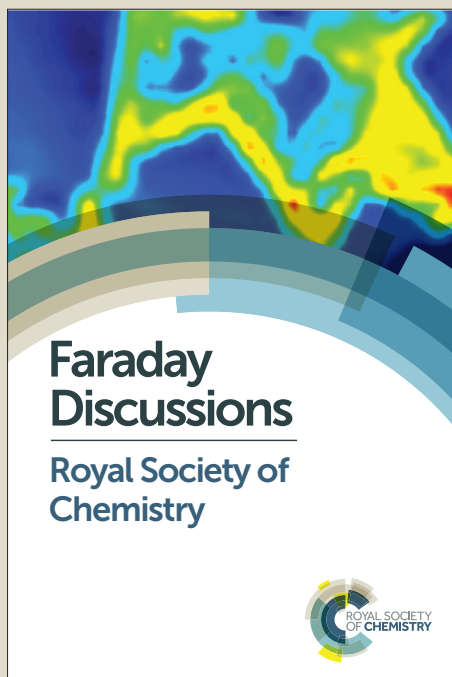
# Faraday Discussions

Accepted Manuscript



This manuscript will be presented and discussed at a forthcoming Faraday Discussion meeting. All delegates can contribute to the discussion which will be included in the final volume.

**Register now to attend!** Full details of all upcoming meetings: <http://rsc.li/fd-upcoming-meetings>



This is an *Accepted Manuscript*, which has been through the Royal Society of Chemistry peer review process and has been accepted for publication.

*Accepted Manuscripts* are published online shortly after acceptance, before technical editing, formatting and proof reading. Using this free service, authors can make their results available to the community, in citable form, before we publish the edited article. We will replace this *Accepted Manuscript* with the edited and formatted *Advance Article* as soon as it is available.

You can find more information about *Accepted Manuscripts* in the [Information for Authors](#).

Please note that technical editing may introduce minor changes to the text and/or graphics, which may alter content. The journal's standard [Terms & Conditions](#) and the [Ethical guidelines](#) still apply. In no event shall the Royal Society of Chemistry be held responsible for any errors or omissions in this *Accepted Manuscript* or any consequences arising from the use of any information it contains.

# **Non-invasive Chemically Specific Measurement of Subsurface Temperature in Biological Tissues using Surface Enhanced Spatially Offset Raman Spectroscopy**

Benjamin Gardner<sup>1)</sup>, Nicholas Stone<sup>1)\*</sup>, Pavel Matousek<sup>2)\*</sup>

1) Biomedical Physics, School of Physics, College of Engineering, Mathematics and Physical Sciences, University of Exeter, Exeter, United Kingdom.

2) Central Laser Facility, Research Complex at Harwell, STFC Rutherford Appleton Laboratory, Harwell Oxford, OX11 0QX, United Kingdom

\*Joint senior and corresponding authors:

**Key words:** Spatially offset Raman spectroscopy, anti-Stokes, temperature, subsurface, non-destructive, non-invasive, SERS, SESORS, T-SESORS

## **Abstract**

Here we demonstrate for the first time the viability of characterising noninvasively the subsurface temperature of SERS nanoparticles embedded within biological tissues using spatially offset Raman Spectroscopy (SORS). The proposed analytical method (SESORS) is applicable in general to diffusely scattering (turbid) media and features high sensitivity and high chemical selectivity. The method relies on monitoring the Stokes and anti-Stokes bands of SERS nanoparticles in depth using SORS. The approach has been conceptually demonstrated using a SORS variant, transmission

Raman spectroscopy (TRS), by measuring subsurface temperatures within a slab of porcine tissue (5 mm thick). Root-mean-square-errors (RMSEs) of 0.20 °C, were achieved when measuring temperatures over ranges between 25–44 °C. This unique capability complements the array of existing, predominantly, surface based temperature monitoring techniques. It expands on a previously demonstrated SORS temperature monitoring capability by adding extra sensitivity stemming from SERS to low concentration analytes. The technique paves the way for a wide range of applications including subsurface, chemical specific, non-invasive temperature analysis within turbid translucent media including: the human body, subsurface monitoring of chemical (eg catalytic) processes in manufacture quality and process control and research. Additionally, the method opens prospects for control of thermal treatment of cancer in vivo with direct non-invasive feedback on temperature of mediating plasmonic nanoparticles.

### **Introduction**

The measurement of subsurface temperature in turbid media is a topical area in analytical sciences with potential applications ranging from monitoring subsurface temperatures in the human body, in vivo, during hyperthermia treatments for cancer; to monitoring chemical and materials processes during production and storage. Current mainstream methods, such as contact thermometers and infrared probes, are confined to measuring the surface temperature in non-IR transparent or diffusely scattering media<sup>1</sup>. There are only a handful of methods capable of measuring temperature at depth in turbid media. Microwave based temperature sensing can penetrate deep inside turbid media; although these sensors have limited spatial resolution due to the long wavelength

of radiation used and do not provide high selectivity to chemical subcomponents<sup>2</sup>. Another approach to deep temperature measurement is Magnetic Resonance Imaging (MRI) thermometry<sup>3</sup>. However as this is reliant upon temperature dependant water proton resonance frequency shifts, this mechanism is not always applicable. There are other temperature dependent properties that can be probed with MRI, such as  $T_1$  (spin-lattice) relaxation time and  $T_2$  (spin-spin) relaxation time of water molecules. Both of these approaches are complex to accurately calibrate, and are limited to specific tissue types<sup>3</sup>. In addition, MRI methods are often prohibitively costly for many practical applications.

Recently we have demonstrated a new approach<sup>4</sup> combining conventional anti-Stokes to Stokes temperature monitoring capability of Raman spectroscopy with subsurface capability of Spatially Offset Raman Spectroscopy (SORS)<sup>5,6</sup> - Temperature SORS (T-SORS). The concept is based on the SORS capability to non-invasively analyse the chemical composition of stratified turbid media. It overcomes the limitation of conventional Raman spectroscopy to near surfaces within diffusely scattering samples.

In general, SORS itself opened a way for a host of new applications including the scanning of liquids in sealed bottles in aviation security, the monitoring of final products and incoming raw materials in pharmaceutical quality control and also paved the way for non-invasive breast cancer and bone disease diagnosis.<sup>7,8</sup> The principle of T-SORS relies on the measurement of both the Stokes and anti-Stokes scattering spectrum of subsurface components using SORS. The temperature is derived from the ratio of the intensities of counterpart Stokes and anti-Stokes lines<sup>9,10</sup>. The ratio is

temperature dependent due to the fact that anti-Stokes Raman bands are solely due to vibrationally excited molecules whereas the Stokes lines derive their intensity from molecules both in the ground as well as vibrationally excited states<sup>4</sup>. In the first proof-of-concept study<sup>4</sup>, the temperatures of a turbid sub-layer of polytetrafluoroethylene (PTFE) was determined through a highly diffusely scattering overlayer of polyoxymethylene POM (3 mm thick) using the intensity ratios of the anti-Stokes and Stokes bands of sublayer (PTFE) recovered non-invasively using SORS measurements. Using calibration data set obtained *a priori* it was possible to predict the sublayer temperature with an accuracy of +/- 0.16 °C over a clinically relevant range of 36-39 °C. The laser excitation wavelength was 830 nm and a standard Raman detection system was used.

Here we expand on the capability of the concept into another related area by demonstrating its viability in monitoring imbedded SERS nanoparticles using SORS in a modality termed – T-SESORS. In a similar way to its earlier counterpart the T-SESORS approach relies on measuring the anti-Stokes to Stokes line of molecules attached or adjacent to SERS nanoparticles (Figure 1) dispersed in sample. This also provides a unique sensing capability enabling probing of the local environment of these particles rather than the bulk subsurface environment derivable from conventional T-SORS. This feature, can be beneficial, for example, in monitoring the temperature of cells adjacent to SERS nanoparticles with high sensitivity stemming from the large enhancement of SERS effect one typically encounters. As such this approach could also be combined with plasmonic photo-thermal therapy<sup>11</sup> where the nanoparticles labelled with antibodies are selectively attached to cancer cells. These then could be used both to

absorb laser radiation to elevate their local temperature and destroy surrounding cancer cells and at the same time to report back on their local environment temperature via the T-SESORS mechanism. This would permit the optimisation of treatment for the most effective cancer eradication whilst minimising collateral damage to healthy cells further away.

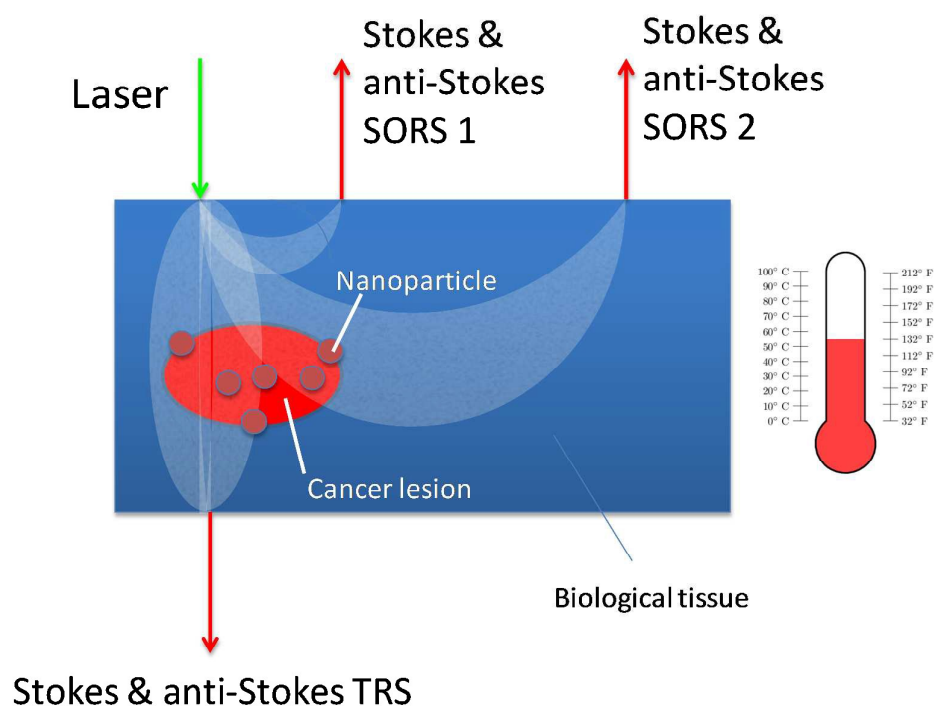


**Figure 1** Schematic diagram of T-SESORS thermometry concept. Both the SORS and TRS geometries permit subsurface monitoring of sample temperature mediated by SERS nanoparticles embedded in turbid medium. The temperature of nanoparticles can also be elevated above background levels and monitored using laser radiation in plasmonic photo-thermal therapy for the most optimum treatment.

## Experimental

The experiments were carried out using a home built instrument based around a transmission Raman geometry<sup>12,13</sup>. Transmission Raman spectroscopy represents a variant of Spatially Offset Raman Spectroscopy (SORS) with the spatial offset present in TRS being at the extreme – ie the illumination zone is on the other side of the sample to the collection zone. Both the geometries achieve subsurface monitoring capability in a comparable manner; with TRS the sensing is biased towards the centre of sample by default whereas with SORS the exact choice of offset defines the penetration depth. With either of the approaches, irrespective of their exact geometry, the detection of distinct subsurface chemical signatures within the sample is the key prerequisite and common feature enabling the unique identification of the temperature of subsurface entity. The basic setup was described earlier<sup>14</sup>. The excitation wavelength was 830 nm and was delivered by a spectrum-stabilised laser (Innovative Photonic Solutions: I0830MM0350MF-EM) passed through two 830 nm band pass filters (Semrock) to clean up the beam profile. Raman spectra were collected on a deep depletion CCD camera (Andor iDus-420) coupled to a Kaiser spectrometer (Holospec 1.8i). All Raman spectra were collected for a total of 5s.

SERS nanoparticles were produced following a previously described method<sup>15</sup>. 1 ml of 0.05 mg ml<sup>-1</sup> nanoparticle (nanoComposix) (60 & 100 nm diameters) and 100 µl of 1 mM SERS thiol based reporter were mixed for 5 minutes. Following mixing the sample was centrifuged at 3,000 rpm for 10 minutes, the supernatant was removed and the nanoparticles re-suspended in 1 ml of phosphate buffered saline (PBS) solution.

The sample consisted of a quartz cell containing the SERS nanoparticles being surrounded by a layer of porcine tissue, the total thickness of the sample was ~10 mm. The sample was kept in a large quartz cell filled with water which was thermostatically controlled by a Thermo Scientific (Haake C10 water bath) coupled to a copper water block.

The experiments were carried out between 25–42 °C, with the temperature increased in increments of ~3.5°C. The temperature was allowed to equilibrate for 40 minutes prior to spectral acquisitions. At each temperature the sample was measured for 40 minutes, generating 480 spectra.

Temperature was measured from the sample in the quartz cell by two type K thermocouples connected to a Pico - TC-08 Thermocouple Data Logger. The temperature was measured every second during measurements and the average temperature over the two thermocouples was used.

The data was analysed using Matlab 2014a, both by fitting a Gaussian curve to either of the chosen SERS bands at 1085 and 1580  $\text{cm}^{-1}$  and when using the partial least-squares regression (PLS) approach. The PLS models were created from every other data point, and validated with the second half (test set), except when otherwise stated.

## Results and Discussion

In SESORS measurements Raman spectra are collected from the sample surface at locations that are separated from the laser illumination point (see Figure 1). The larger



the separation (spatial offset  $\Delta s$ ) the larger the contrast between the sublayers and surface layers. Two or more spectra would typically be collected and processed using scaled subtraction or a larger number acquired and processed using multivariate analysis to recover the estimates of pure spectra of individual layers. In the transmission configuration, bulk information within the probe volume can be obtained and subsurface temperature from any subsurface regions with distinct Raman signatures recovered in a single measurement. Figure 2 presents a schematic diagram of the experimental setup for temperature measurements used here, in which the sample is probed in transmission geometry.

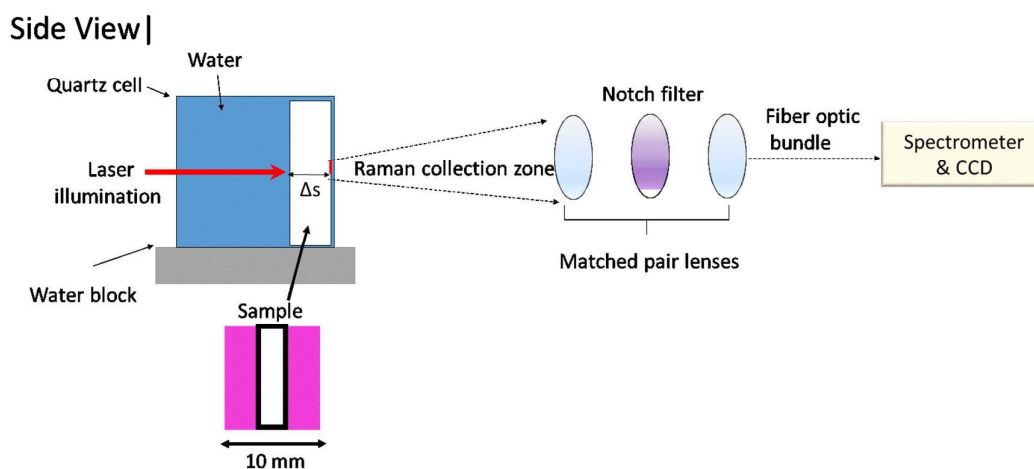


**Figure 2 | Schematic of the experimental setup.** The 830 nm laser beam is passed through the sample in transmission geometry. The sample consists of two layers of porcine meat, one on either side (wrapped around) of a quartz cell containing SERS nanoparticles. The Raman photons are collected by a 50 mm diameter  $f=60$  mm lens,

filtered by a Kaiser notch filter (830 nm), focussed with a 50 mm diameter  $f=60$  mm lens onto a fibre bundle (Ceramoptec). The circular cross-section fibre bundle is rearranged into a line of fibres matching entry into a Kaiser Holospec 1.8i spectrometer with a low dispersion transmission grating and an Andor iDus 420 deep depletion CCD.

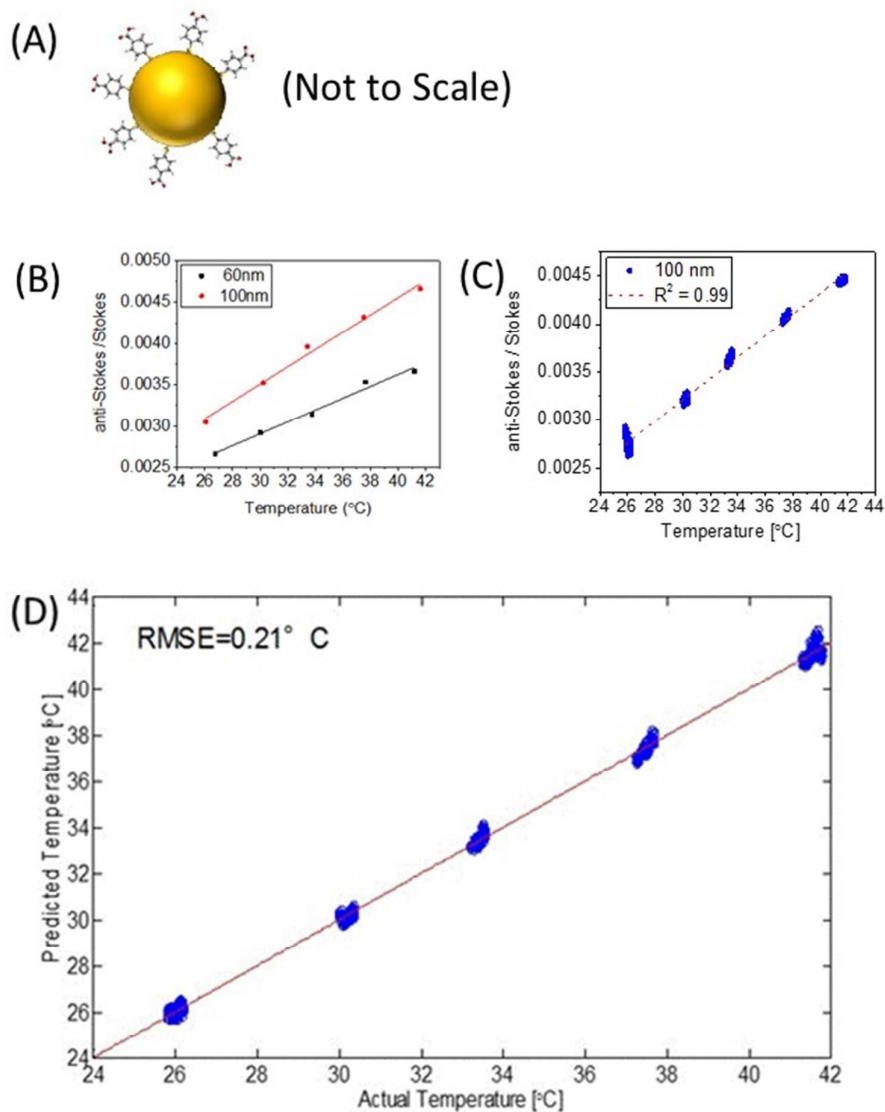


**Figure 3| Testing of T-SERS concept using non-buried SERS nanoparticles.** **A**, illustration of the thiol attachment of the chosen SERS reporter to the gold nanoparticles. **B**, anti-Stokes / Stokes ratio of a chosen Raman band ( $1580\text{ cm}^{-1}$ ) for two nanoparticle sizes (60 & 100 nm). **C**, univariate model for predicting temperature for 100 nm SERS nanoparticle based upon anti-Stokes/Stokes of the  $1580\text{ cm}^{-1}$  peak. **D**, Performance of PLS model for predicting temperature of SERS nanoparticle.

The general viability of using SERS as temperature reporters has been established earlier<sup>16</sup>. In a first set of experiments we have confirmed that the nanoparticles selected for non-invasive studies here are also viable for monitoring temperature using the Stokes and anti-Stokes signals (Figure 3). A solution with dispersed nanoparticles has been placed in a plastic tube and measured directly in transmission across a temperature range of 25–42 °C. It should be noted that the ratio of anti-Stokes to Stokes Raman bands, in general, is not a linear function of temperature as the dependence involves an exponential function<sup>4</sup>. However across a relatively narrow range of temperatures as used here the linear approximation of the dependence is entirely adequate as demonstrated. (If a wider range of temperatures was monitored where nonlinear dependence was revealed in the calibration stage then a non-linear univariate or multivariate analysis could be invoked and used to fit the calibration data and then predict unknown temperatures.)

Due to differences in the SERS enhancement as a function of nanoparticle diameter (as expected) there are also differences in the anti-Stokes/Stokes ratio of the chosen Raman band at  $1580\text{ cm}^{-1}$  (Figure 3B) at the same temperature. Through using the univariate

analysis approach, i.e. monitoring the ratio between the anti-Stokes/ Stokes ratio, it was possible to create a model and predict the temperature with the test set. As is shown (Figure 3C) with the 100 nm nanoparticles an RMSE of 0.43 °C was achieved, and a similar value was also achieved with the 60 nm particles (data not shown).

To further explore the limits of the technique and reach higher accuracies we deployed a multivariate analysis using the entire spectral range measured in both the Stokes and anti-Stokes spectral regions. A PLS model has been constructed to predict temperature from a calibration data set (Figure 3D). The model yielded an RMSE of 0.21 °C, about twice as accurate than the basic univariate approach above.

The concept of T-SESORS has been demonstrated initially on a quartz vial containing a solution with nanoparticles dispersed within it, concealed behind a total of 5 mm thick layer of porcine tissue (~2.5 mm on each side). The Raman spectra of the nanoparticles and the signal when buried in porcine tissue are shown in Figure 4.

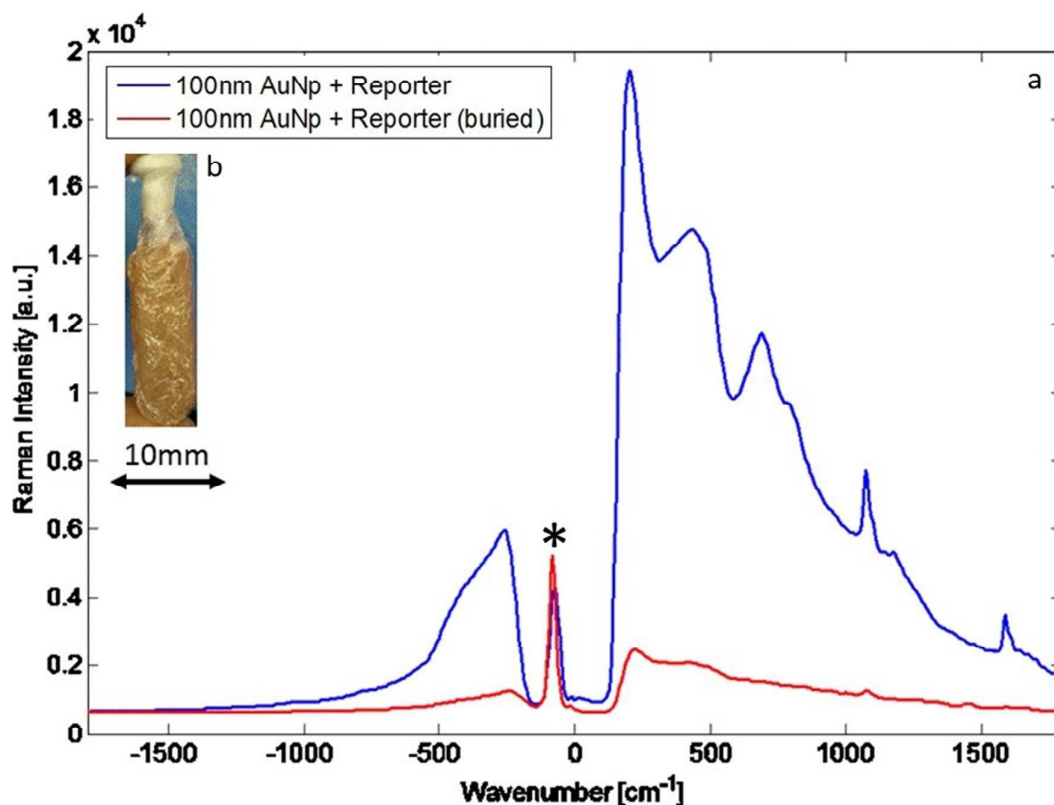


**Figure 4 | Anti-Stokes and Stokes Raman spectra of gold nanoparticles alone + buried in porcine.** a, the Raman spectra of the SERS signal when measured in a quartz cell (blue), and when the cell is buried in porcine tissue (red). b, the quartz cell wrapped around with porcine tissue. An artefact due to the elastically scattered and unfiltered laser line is labelled with asterisk.

The spectra were measured at different temperatures in a clinically relevant range of 25–42 °C. The data were split into calibration and prediction data sets, both contained half the measured data.

Again a univariate analysis was performed on a SERS band ( $\sim 1085\text{ cm}^{-1}$ ), the average of which is shown for the anti-Stokes and Stokes intensities respectively for each

measured temperature (Figure 5a). A calibration curve was produced (Figure 5b), which achieved a prediction error (RMSE) of 1.4 °C (Figure 5c). An unusual phenomenon was observed at the Stokes Raman band (Figure 5a - right panel), which was decreasing in intensity with increasing temperature. This phenomenon was not observed for SERS nanoparticles alone suggesting that the absorption or scattering properties of surrounding tissue are changing with temperature and causing this trend. (It should be noted that this had no impact on the accuracy or performance in general of both the univariate and multivariate methods as the effect is accounted for in the calibration stages with both the approaches.)

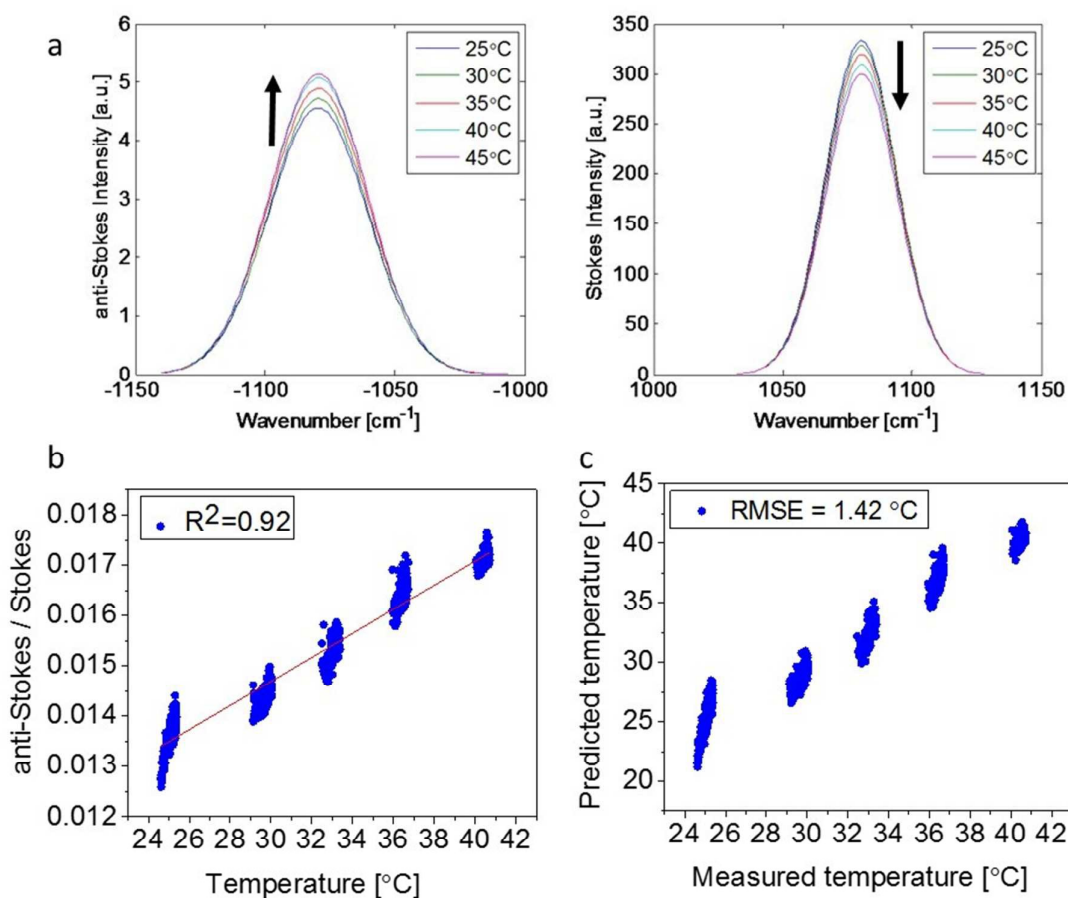


**Figure 5 | Univariate temperature monitoring of burried gold nanoparticles.** a, the average anti-Stokes & Stokes band of the SERS Raman reporter ( $\sim 1080\text{ cm}^{-1}$ ) at each temperature point. b, calibration curve of the SERS reporter. c, correlation between the measured temperature and the predicted temperature on a prediction (test) sample.

As above we have also applied a multivariate analysis to the problem to derive a higher predictive accuracy. In constructing a PLS model it is crucial to select the optimal number of components, too few and the model could be underfit, while too many can lead to overfitting, either of which can lead to a poor predictive ability with future

samples. The full spectral range of was used in a PLS model to create a model and predict unknown temperatures, the results of which are shown in Figure 6. Here a leave-every other-replicate-out PLS model was constructed from the experimental data, the number of PLS components versus the percentage of explained variance (Fig. 6a) shows that most of the variance is explained within the first 5 components. The model constructed using PLS (Figure 6b) showed an improved  $R^2$  in comparison to that achieved through the univariate approach (0.99 vs 0.92). More importantly though there was an improvement in the prediction power with a decrease in the RMSE from 1.4°C to 0.20°C.



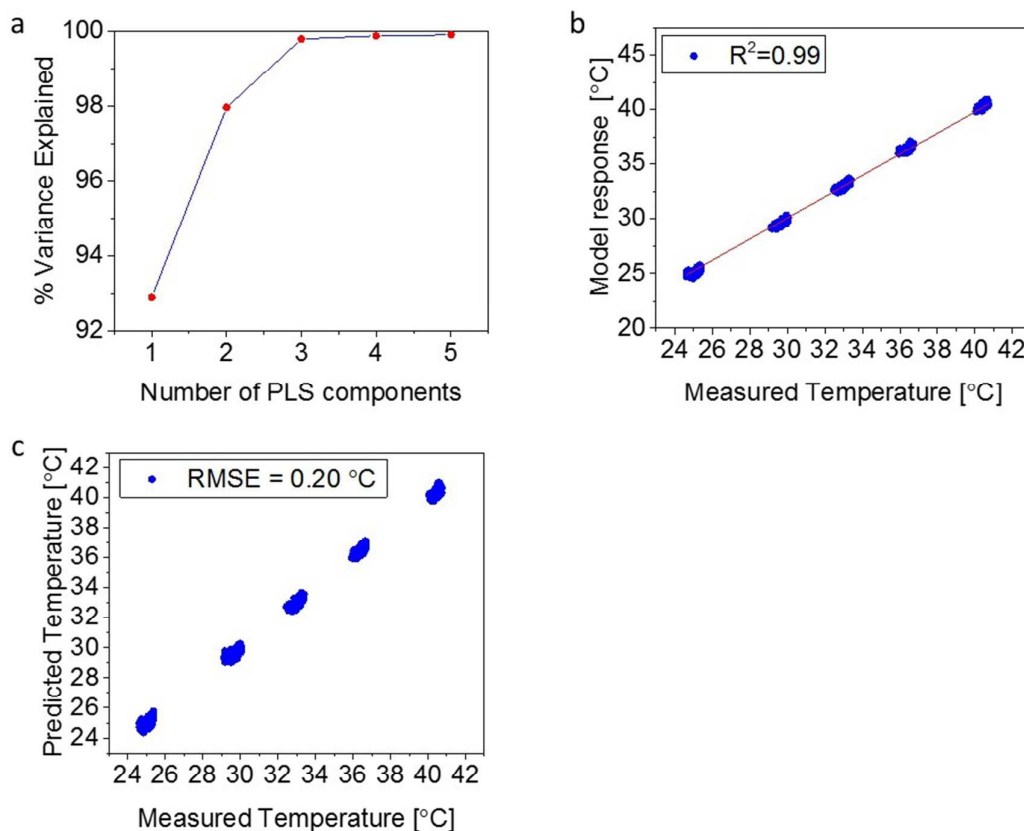


**Figure 6 | PLS Model of heating buried nanoparticles (25–42 °C).** **a**, the percentage of variance explained for the model data, as a function of the number of components used in the PLS model of nanoparticles being heated in a layer of porcine. **b**, the fit response vs observed response for the PLS model (calibration data set). **c**, Predicted temperatures vs the measured temperature for nanoparticles in porcine for the final test set of data (prediction data set).

To further explore the limits of T-SESORS, a thicker layer of porcine was introduced, 10 mm thickness in total with the cell buried in the middle. By doubling the thickness of the tissue layer there was a small increase in the level of error (Figure 7), with small increase in the RMSE from 0.20 to 0.23 °C in the PLS model.

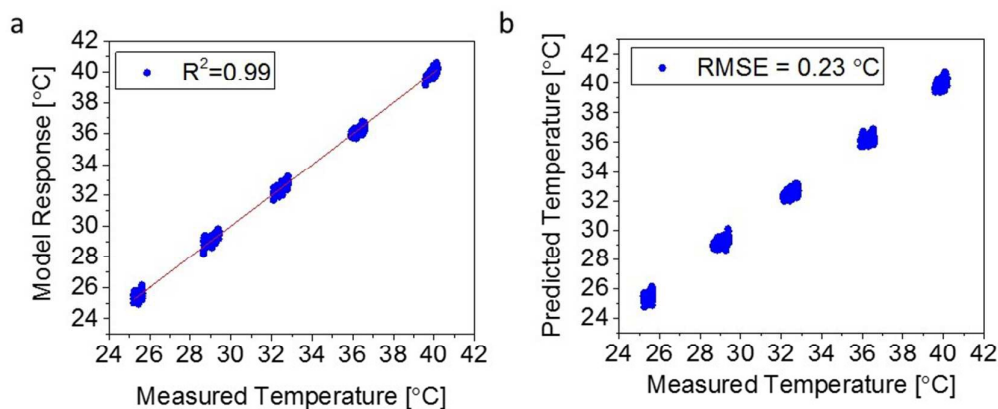


**Figure 7 | PLS Model of heating buried nanoparticles (25–42 °C) 10 mm porcine.** a, the fit of the model response and the measured temperature. b, predicted temperatures vs the measured temperature of the gold nanoparticles.

It should be noted that further optimisation of the technique is envisaged by improving data pre-processing and experimental apparatus. The results presented here represent only the first conceptual demonstration of T-SESORS.

An important practical aspect of these measurements is how to derive appropriate calibration T-SESORS data at different temperatures to enable the prediction of unknown temperature from T-SESORS spectra. In situations, where invasive access to the sample can be facilitated, e.g. in some industrial process control situations, this is relatively straightforward and subsurface calibration temperature can easily be ascertained. In many situations, however, this may not be possible. In such cases an alternative option exists consisting of acquiring calibration spectra from a sample that is

in full thermal equilibrium with its environment, i.e. ensuring any thermal gradients are absent during the calibration measurements. In such situation the subsurface temperature can be assumed to be the same as that of the sample surface and simply acquired from a surface measurement. By altering the temperature of the ambient environment and letting the sample to equilibrate fully again additional T-SORS spectra at different temperatures can be further acquired if desired, or necessary. In most situations where a specific anti-Stokes Raman spectra region is known how it responds to temperature (response curve slope) only one calibration data point (temperature) may be required to compensate for any absorption within the sample that could distort true anti-Stokes to Stokes band ratios in a specific sample and experimental geometry. In biomedical field this could be the normal (equilibrated) body temperature.

### **Conclusions**

Here we have demonstrated for the first time the viability of T-SESORS, a new technique for monitoring noninvasively the temperature of sub-surface turbid materials with imbedded SERS nanoparticles within it as temperature reporters. The development of a method for non-invasive measurement of temperature at depth, has practical applications in a variety of fields including biomedical monitoring, catalytic research and process monitoring. Apart from monitoring temperature in depth in samples with static thermal gradients the method also enables the measurements of non-equilibrated systems where chemically distinct entities are at different temperatures from their surroundings and their temperature evolves in time (eg a chemical reaction in progress with direct monitoring of reagents or catalysts). In addition the concept is also potentially useable in hyperthermia cancer treatments using nanoparticles, by providing

a direct means of monitoring the temperature of plasmonic nanoparticles by non-invasive means.

### Acknowledgements

An EPSRC grant (EP/K020374/1) partly funded the work presented here.

### References

1. P. R. N. Childs, J. R. Greenwood and C. A. Long, *Rev. Sci. Instrum.*, 2000, **71**, 2959-2978.
2. A. Levick, D. Land and J. Hand, *Meas. Sci. Technol.*, 2011, **22**, 065801.
3. K. Hynynen, N. McDannold, R. V. Mulkern and F. A. Jolesz, *Magn. Reson. Med.*, 2000, **43**, 901–904.
4. B. Gardner, P. Matousek and N. Stone, *Anal. Chem.*, 2015, DOI: 10.1021/acs.analchem.5b03360.
5. P. Matousek, I. P. Clark, E. R. C. Draper, M. D. Morris, A. E. Goodship, N. Everall, M. Towrie, W. F. Finney and A. W. Parker, *Appl. Spectrosc.*, 2005, **59**, 393–400.
6. P. Matousek, M. D. Morris, N. Everall, I. P. Clark, M. Towrie, E. Draper, A. Goodship and A. W. Parker, *Appl. Spectrosc.*, 2005, **59**, 1485–1492.
7. K. Buckley and P. Matousek, *Analyst*, 2011, **136**, 3039-3050.
8. P. Matousek and N. Stone, *Chem. Soc. Rev.*, in press, DOI: 10.1039/c5cs00466g
9. H. Baokun, T. Yanjie, L. Zuowei, G. Shuquin and L. Zhaokai, *Instrum. Exp. Tech.*, 2007, **50**, 282-285.

- 
10. E. Smith and G. Dent, *Modern Raman Spectroscopy – A Practical Approach* Ch. 6, (John Wiley & Sons Ltd, Chichester 2005).
  11. X Huanga and M.A. El-Sayed, *Alex. J. Med.*, 2011, **47**, 1–9.
  12. B. Schrader and G. Bergmann, *Zeitschrift fur Analytische Chemie Fresenius*, 1967, **225**, 230.
  13. P. Matousek and A.W. Parker, *Appl. Spectrosc.*, 2006, **60**, 1353-1357.
  14. M. Z. Vardaki, B. Gardner, N. Stone and P. Matousek, *Analyst*, 2015, **140**, 5112–5119.
  15. A. Jaworska, L.E. Jamieson, K. Malek, C.J. Campbell, J. Choo, S. Chlopicki and M. Baranska, *Analyst*, 2015, **140**, 2321-2329.
  16. E.A. Pozzi, A.B. Zrimsek, C.M. Lethiec, G.C. Schatz, M.C. Hersam and R.P. Van Duyne, *J. Phys. Chem. C*, 2015, **119**, 21116–21124.